BLIND IDENTIFICATION OF SEF DYNAMICS FROM MEG DATA BY USING DECORRELATION METHOD OF ICA

Kuniharu $Kishida^1$, *Kenji* $Kato^1$, *Kazuhiro* $Shinosaki^2$, *Satoshi* $Ukai^2$

[1]Faculty of Engineering, Gifu University, Gifu 501-1193, Japan
[2]Osaka University Graduate School of Medicine, Osaka 565-0871, Japan
E-mail: kishida@cc.gifu-u.ac.jp; kato@ksd.info.gifu-u.ac.jp
{sinosaki, ukai}@psy.med.osaka-u.ac.jp

ABSTRACT

A new way of dynamical understanding of brain function of somatosensory evoked magnetic fields (SEF) is proposed by using the decorrelation method of independent component analysis (ICA) and our blind identification method of transfer functions based on feedback system theory. Magnetoencephalography (MEG) data are analyzed at special frequency by the decorrelation method of ICA, and two components that have dipole-type of patterns on scalp are selected. Taking the inverse ICA from two components we can have time series data oriented to SEF. From SEF time series data transfer functions between two regions on scalp can be obtained by using blind identification method based on feedback system theory. Impulse responses between main brain region of SEF and the other region in opposite hemispheric is analyzed. Their directional dependence is found.

1. INTRODUCTION

It is important to have dynamical understanding of brain function between inter-cortexes. A new approach for brain dynamics of SEF will be introduced in the present paper. Via the decorrelation method of ICA SEF dynamics is studied by our identification method of transfer functions based on feedback system theory [1] [2].

By the decorrelation method of ICA [3] [4] [5], it will be discussed in Sect. 4 that two components which have dipole-type of patterns on scalp are selected from MEG data. Taking the inverse ICA from two components we will obtain time series data oriented to SEF. Then, transfer functions between two regions on scalp will be obtained from SEF time series data by using our blind identification method based on feedback system theory, and their impulse response will be obtained in Sect.5.

2. SOMATOSENSORY EVOKED MAGNETIC FIELDS

Electric stimulation to any part of the body evokes a cortical SEF. In clinical studies, the median nerve at the wrist is usually stimulated. Recent studies of SEFs detected by averaging MEG have identified dipole sources activated in sensory cortices after median nerve stimulation. The averaged MEG contain four main peaks within the first 100 msec after the median nerve stimulation as will be shown in Fig. 1. A number of investigators consider the cortical response at the earliest peak with the large amplitude to represent activation of pyramidal cells in the posterior wall of the central sulcus, i.e. area 3b (Brodmann) of the primary somatosensory cortex (SI) in the contralateral hemisphere [6] [7], while the sources of the latter components remain controversial.

First author thanks for Grant Aid for Scientific Research (No.14580346) of Japan society of the Promotion of Science.

3. MEG RECORDINGS AND ANALYSIS

Subject was a 32-year-old healthy male volunteer. The right median nerve was stimulated electrically with a constant-voltage, square-wave pulse of 0.2 msec duration delivered transcutaneously at the wrist. Stimulus frequency was 5Hz, and stimulus intensity was adjusted to the lowest level that would produce a twitch of the thumb. SEFs were recorded with a 64-channel whole-head MEG system equipped with third-order SQUID gradiometers (NeuroSQUID Model 100; CTF Systems Inc., Port Coquitlam, Canada). The location of SQUID channels will be shown in Fig. 7. MEG signals were digitized at 1250 Hz and filtered with a 300 Hz low-pass filter. Data of 200 msec duration including a 100 msec pre-stimulus interval were recorded for each of 500 trials and analyzed off-line as a single sweep. Preset notch filters were used at 60, 120 and 180Hz. Averaged MEG is shown in Fig. 1, and its isofield map of the third time peak is shown in Fig. 2. In Fig. 2, positive and negative values are drown by solid and broken lines, respectively. These results are obtained by the conventional approach in MEG analysis.

4. DECORRELATIOM METHOD OF ICA

In MEG signals it is useful to use the second-order correlations for these periodic types of source separation, so called decorrelation method, since we want to isolate only components of 5Hz SEF, which have specific time structures. The decorrelation method was developed by Molgedey and Schuster [3], Murata, et al. [5], and briefly summarized in [2]. We have tried the blind source separation (BSS) method

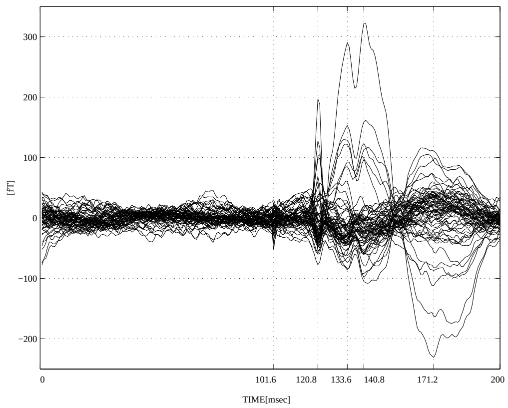

Fig. 1. Averaged MEG of $\boldsymbol{y}$. (Stimulus time is 0.1016.)

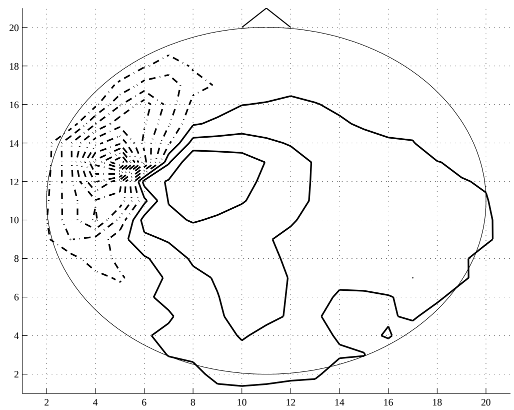

Fig. 2. Isofield map of the third time or largest peak.

based on temporal structure to separate components related to SEF. In the BSS method, we assume that single sweep MEG signals, $\boldsymbol{y}(n) = (y_1(n), \ldots, y_{64}(n))^{\mathrm{T}}$ at discrete time n, consist of underlying sources $\boldsymbol{s}(n) = (s_1(n), \ldots, s_{64}(n))^{\mathrm{T}}$ which are mutually statistically independent, and that the sources are mixed by an linear mixing process $\boldsymbol{A}$ as

$$\boldsymbol{y}(n) = \boldsymbol{A}\boldsymbol{s}(n), \tag{1}$$

where each component s_i has zero mean. In the BSS method L correlation matrices, $M(\tau_k) = \frac{1}{N}\sum_{n=1}^{N} \tilde{\boldsymbol{y}}(n)\tilde{\boldsymbol{y}}(n+\tau_k)^T$ $(k = 1, 2, \ldots, L)$, are diagonalized simultaneously, where $\tilde{\boldsymbol{y}}$(n) is the orthonormalized vector of $\boldsymbol{y}$(n) and τ_k is defined by

$$\tau_k = \left[\frac{1250k}{5}\right], \quad k = 1, 2, \ldots, L. \tag{2}$$

Here $[\cdot]$ rounds the value to nearest integer. To solve approximately this simultaneous diagonalization problem, a Jacobi-like algorithm proposed by Cardoso and Souloumiac [8] was used. In our case, we have obtained good results for $L = 3$.

After we have found the mixing matrix $\boldsymbol{A}$, we can obtain independent components (ICs) by calculating $\boldsymbol{s}(n) = \boldsymbol{A}^{-1}\boldsymbol{y}(n)$. Hence 64ch MEG data can be decomposed into

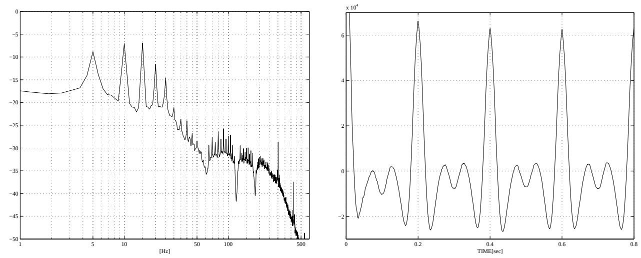

(a) PSD of s_7 (b) Autocorrelation of s_7

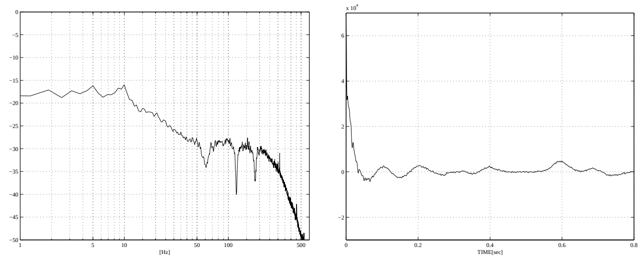

(c) PSD of s_{14} (d) Autocorrelation of s_{14}

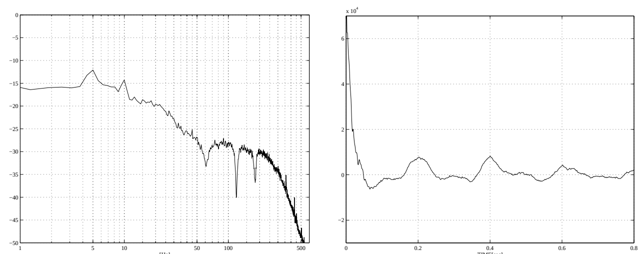

(e) PSD of s_{26} (f) Autocorrelation of s_{26}

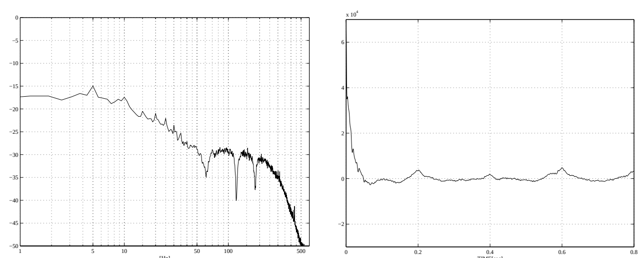

(g) PSD of s_{29} (h) Autocorrelation of s_{29}

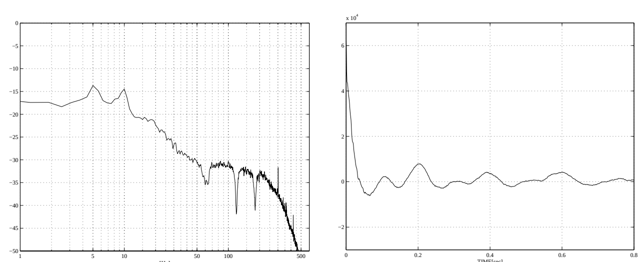

(i) PSD of s_{39} (j) Autocorrelation of s_{39}

Fig. 3. AutoPSDs and autocorrelation functions of five ICs, $s_7(n)$, $s_{14}(n)$, $s_{26}(n)$, $s_{29}(n)$, and $s_{39}(n)$, related to 5Hz periodical stimulus. Amplitude of PSD is the decibel representation. The other 59 ICs have no peak at 5Hz in their PSDs.

64 ICs. The mixing matrix A and ICs were estimated by using the decorrelation method. We selected five ICs related to 5Hz SEF, $s_7(n)$, $s_{14}(n)$, $s_{26}(n)$, $s_{29}(n)$, and $s_{39}(n)$, from their power spectral density function (PSD) and autocorrelation functions, which are shown in Fig. 3.

MEG time series data related to 5Hz SEF, $\boldsymbol{s}_{5sef}(n) := (s_7(n) s_{14}(n)\ s_{26}(n)\ s_{29}(n)\ s_{39}(n))^T$, could be obtained by $\boldsymbol{y}_{5sef}(n) = \boldsymbol{A}_{5sef}\boldsymbol{s}_{5sef}(n)$, where $\boldsymbol{A}_{5sef} := (A_{*,7}\ A_{*,14}\ A_{*,26}\ A_{*,29}\ A_{*,39})$ consists of five column vectors of the mixing matrix $\boldsymbol{A}$. Here $A_{*,i}$ is the i-th column vector of $\boldsymbol{A}$. Averaged MEG of $\boldsymbol{y}_{5sef}(n)$ are shown in Fig. 4. Comparison of Fig. 1 with Fig. 4 shows us that $\boldsymbol{y}(n)$ equals to $\boldsymbol{y}_{5sef}(n)$ in terms of averaged MEG, and that our blind source separation of SEF is successful.

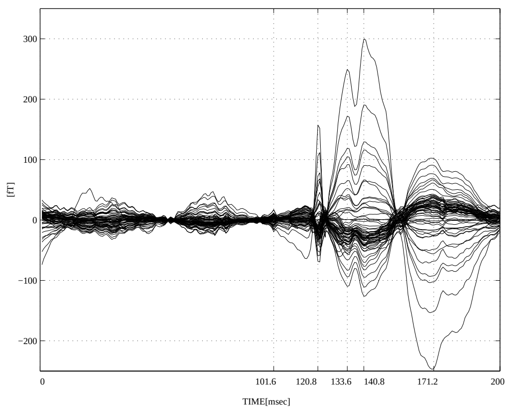

Fig. 4. Averaged MEG of $\boldsymbol{y}_{5sef}$ related to 5Hz ICs.

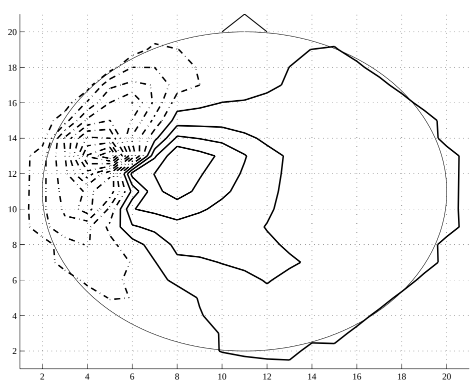

Fig. 5. Isofield map of $A_{*,7}$ corresponding to s_7.

Furthermore, their isofield maps of five ICs were examined to have dipole like patterns as mentioned in [4] [9] [10]. That is, we can have current dipoles which correspond to those of lead fields in a lucky situation. From column vectors $A_{*,7}$ and $A_{*,26}$ those patterns of isofield on scalp are shown Figs. 5 and 6. Comparison of Fig. 5 with Fig. 2 shows us the same isofield map. In Fig. 6 we can find a dipole corresponding to the right hemisphere. Hence, we

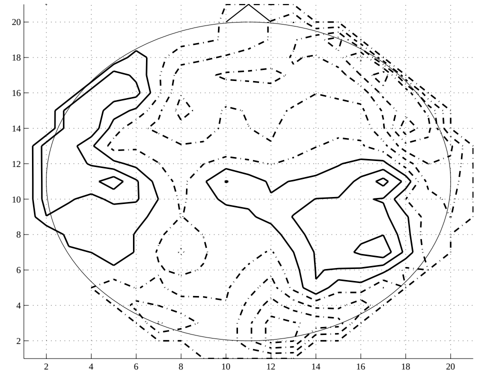

Fig. 6. Isofield map of $A_{*,26}$ corresponding to s_{26}.

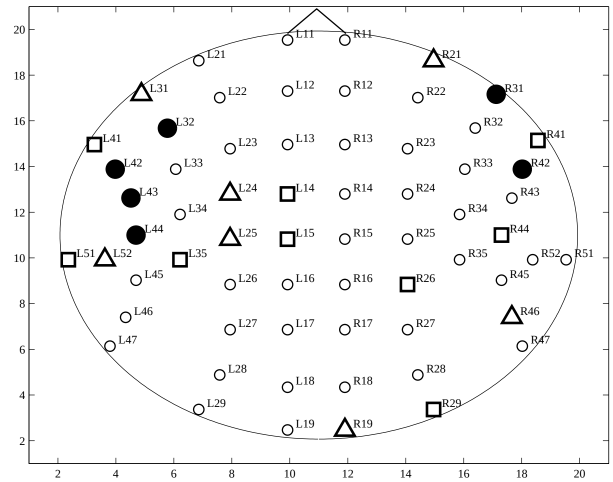

Fig. 7. Location of SQUID channels and PSDs of SEF MEG ($\boldsymbol{y}_{sef}$) related to s_7 and s_{26}.

selected two components of s_7 and s_{26} from five ICs, which have dipole patterns in regions related to somatosensory.

Since we selected two ICs related to 5Hz SEF after the confinement of dipole positions, let us MEG data transformed from two ICs be called SEF MEG data. That is, we have

$$\boldsymbol{y}_{sef}(n) = \boldsymbol{A}_{sef}\boldsymbol{s}_{sef}(n), \tag{3}$$

where $\boldsymbol{s}_{sef}(n) := (s_7(n)\ s_{26}(n))^T$ and $\boldsymbol{A}_{sef} := (A_{*,7}\ A_{*,26})^T$. PSDs of SEF MEG data related to s_7 and s_{26} are shown in Fig. 7. The symbols of $\circ$, $\square$, $\triangle$ and $\bullet$ in figure means very small, small, medium and large absolute values of PSDs at 5Hz. Effects of two dipoles can be shown by the symbols of $\square$, $\triangle$ and $\bullet$ in somatosensory areas of Fig. 7. Hereafter, time series data of SEF MEG, $\boldsymbol{y}_{sef}(n)$, are analyzed in the remaining part of this paper.

For reconfirmation of two dipole patterns of s_7 and s_{26} we calculated two groups of averaged SEF MEG from $\boldsymbol{y}_7(n) := A_{*,7}\ s_7(n)$ and $\boldsymbol{y}_{26}(n) := A_{*,26}\ s_{26}(n)$, and arranged them on scalp as shown in Figs. 8 and 9.

When crosscorrelation functions are obtained from SEF

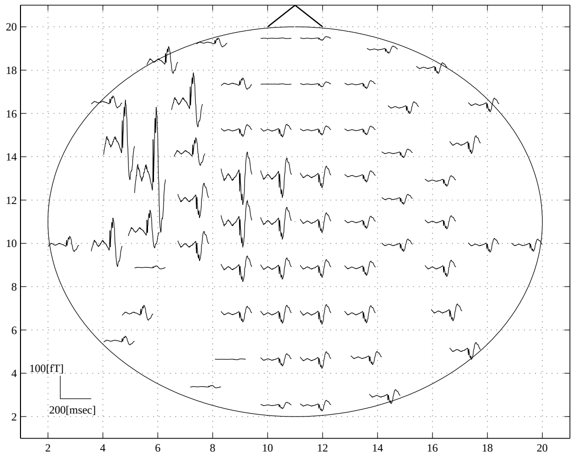

Fig. 8. Averaged MEG of $\boldsymbol{y}_7$ on scalp.

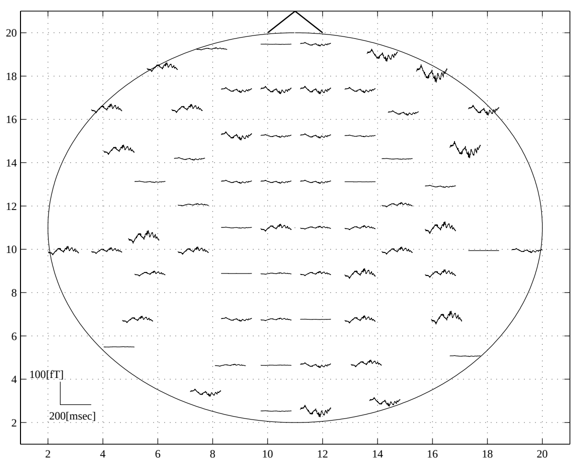

Fig. 9. Averaged MEG of $\boldsymbol{y}_{26}$ on scalp.

MEG time series data, asymmetry of crosscorrelation functions between fixed L43 and some SQUID channels of right hemisphere are shown in Fig. 10. In figure curves show asymmetry of crosscorrelation functions within 80 msec. Effect of dipole is found by comparison of the curve at R42 with that at R44 in right hemisphere.

5. BLIND IDENTIFICATION METHOD BASED ON FEEDBACK SYSTEM THEORY

In our blind identification method of feedback model, it is assumed that there is a Gaussian stationary process of linear feedback part embedded in a complex nonlinear system (see Fig. 11) by cutting high and low frequency interactions [2]. Usually high and/or low pass filters are used for elimination of the interactions. From our blind identification method we can find a linear feedback model given by

$$\begin{aligned} y_i(n) &= F_{ij}(z^{-1})y_j(n) + F_i(z^{-1})f_i(n) \\ y_j(n) &= F_{ji}(z^{-1})y_i(n) + F_j(z^{-1})f_j(n), \end{aligned} \quad (4)$$

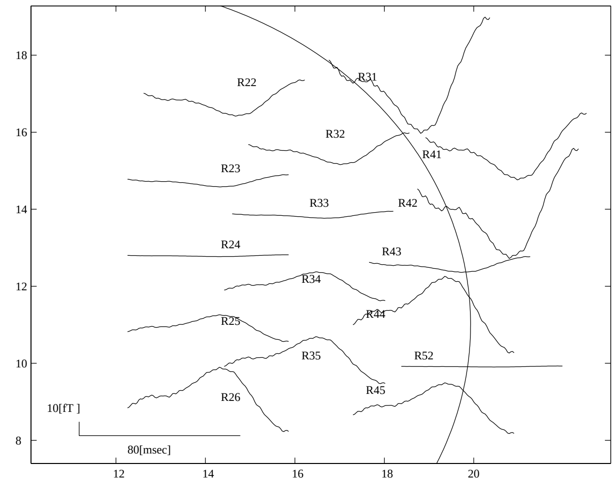

Fig. 10. Asymmetry of crosscorrelation functions between L43 and some SQUID channels of right hemisphere.

where i and j are two integers ($1 \leq i, j \leq 64$ and $i \neq j$), 64 is the number of SQUID channels, $y_i(n)$ and $y_j(n)$ are output variables selected from SEF MEG $\boldsymbol{y}_{sef}$, $f_i(n)$ are Gaussian white random variables with $E\{f_i(n)f_j(m)\} = V_{ij}\delta_{nm}$, and z^{-1} is the backward time shift operator: $z^{-1}y_i(n) = y_i(n-1)$. The stable feedback model has four blocks of open loop transfer functions given as

$$\begin{aligned} F_{ij}(z^{-1}) &:= C_{ij}(I - A_{ij}z^{-1})^{-1}B_{ij}z^{-1} \\ F_i(z^{-1}) &:= C_i(I - A_i z^{-1})^{-1}B_i. \end{aligned} \quad (5)$$

Selecting time series data of $\boldsymbol{y}_{sef}(n)$ instead of $\boldsymbol{y}(n)$ by the BSS method based on the temporal structure corresponds to finding out a part of Eq. (4) from a total system, if the feedback model of the part has a linear Gaussian process.

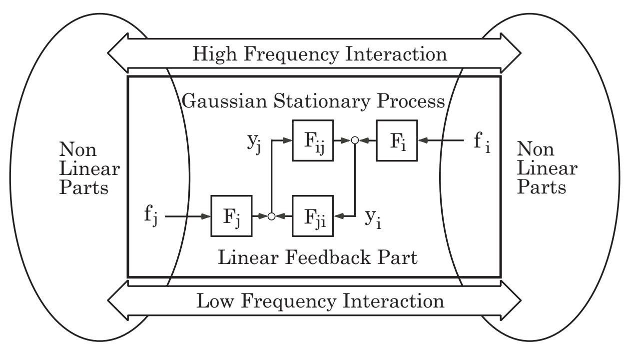

Fig. 11. Linear stochastic feedback model embedded in MEG.

From the viewpoint of stochastic/statistical inverse problems [1] [11] [12] we have discussed a theory of blind identification, and obtained a numerical innovation model equivalently in terms of correlation functions. Let the numerical innovation model of Eq. (4) be identified from $\boldsymbol{y}_{sef}(n)$ as

$$\begin{aligned} x(n|n) &= Ax(n-1|n-1) + B\gamma(n) \\ (y_i(n)\ y_j(n))^T &= Cx(n|n). \end{aligned} \quad (6)$$

where $\gamma(n)$ is an innovation vector which has equivalent random varibales. Coefficient matrices A, B and C of the numerical innovation model should have minimum phase properties of pole stability and zero invertiblity;

$$\mathrm{eig}|A| < 1 \quad \text{and} \quad \mathrm{eig}|A(I - BC)| < 1. \qquad (7)$$

Furthermore, we have described that open loop transfer functions can be obtained from closed loop transfer function matrix, $G(z^{-1}) = C(I - Az^{-1})^{-1}B$ by feedback structure. That is, we have

$$\begin{aligned} \hat{F}_{ij}(z^{-1}) &= G_{ij}(z^{-1})(G_{jj}(z^{-1}))^{-1} \\ \hat{F}_{ji}(z^{-1}) &= G_{ji}(z^{-1})(G_{ii}(z^{-1}))^{-1}. \end{aligned} \qquad (8)$$

where

$$G(z^{-1}) =: \begin{pmatrix} G_{ii}(z^{-1}) & G_{ij}(z^{-1}) \\ G_{ji}(z^{-1}) & G_{jj}(z^{-1}) \end{pmatrix}.$$

Especially, open loop transfer functions between output variables are invariant, if the original feedback system satisfies either sufficient condition: One condition is the minimum phase property or the other is independence of random variables. That is, we can identify correctly open loop transfer functions from the numerical innovation model by using a transformation with feedback structure, if the original model has either sufficient condition. However, it should be noted that its closed loop transfer function matrix from innovations to output variables is not invariant, since the innovations are equivalent random variables. On the other hand, poles of Eq. (6) are invariant, and open loop transfer functions in the feedback model are also invariant, if the original model has above mentioned property.

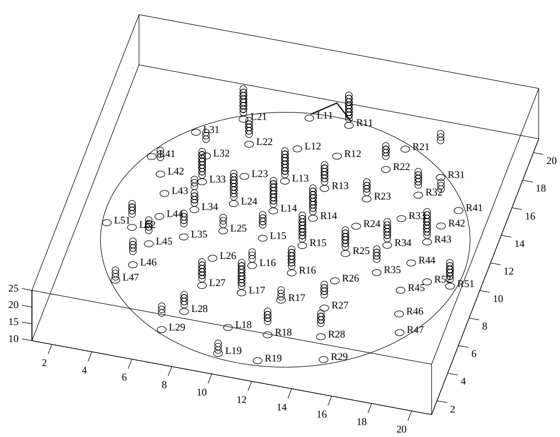

Fig. 12. Minimum phase property of innovation models between L43 and the other SQUID channel.

Open loop transfer functions can be identified by following steps of our blind identification method based on feedback system theory [1] [11] [12]:

a) Correlation function matrices are obtained from stationary Gaussian time series data of $\boldsymbol{y}_{sef}(n)$.

b) By using the singular value decomposition of Hankel matrix, coefficient matrices of numerical innovation model are obtained from Hankel associate matrices after solving a matrix Riccati equation.

c) Minimum phase property of numerical innovation models is checked, and closed loop transfer functions are obtained from numerical innovation models.

d) Open loop transfer functions are obtained by Eq. (8).

e) Model reduction is needed for the open loop transfer functions.

Figure 12 shows us that whether an identified innovation model between L43 and the other SQUID channel is minimum phase or not. In figure the symbol of $\circ$ at a height of m on the other SQUID position means that a numerical innovation model identified from m singular values of Hankel matrix is minimum phase, when we examine a feedback model between y_i of L43 and y_j of the other SQUID channel.

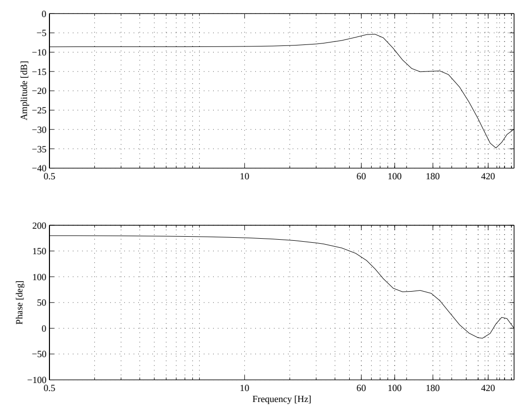

Fig. 13. $F_{12}(z^{-1})$ between R43 and L43.

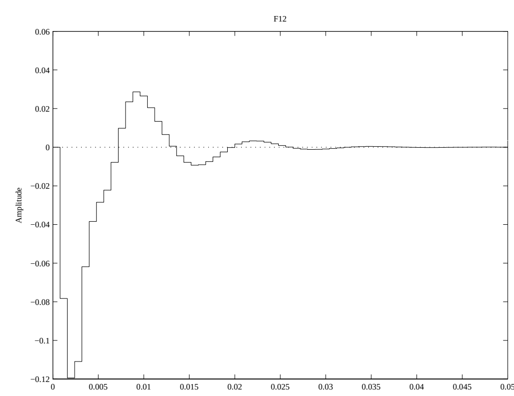

Fig. 14. Impulse response of $F_{12}(z^{-1})$ from R43 to L43.

For channels L43 and R43 of Fig. 12 we obtained a minimum phase innovation model identified from Hankel matrix with 14 singular values, and calculated its closed loop transfer function matrix. From Eq. (8) and suitable model reduction we could have an open loop transfer function with order 6, $F_{12}(z^{-1})$, from R43 to L43 as in Fig. 13, after high harmonics effects of electrical power noise at 300 Hz were omitted. Its impulse response is shown in Fig. 14. Open loop transfer function $F_{21}(z^{-1})$ from L43 to R43 is also shown in Fig. 15 and its impulse response is in Fig. 16.

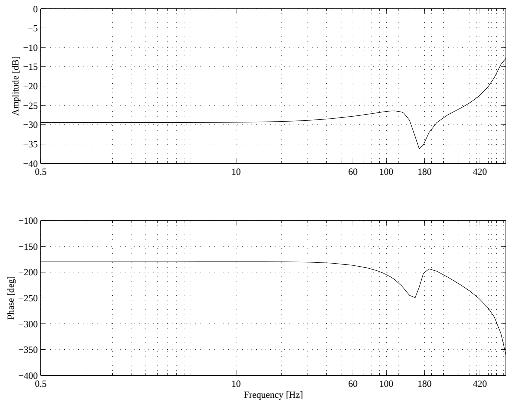

Fig. 15. $F_{21}(z^{-1})$ between L43 and R43.

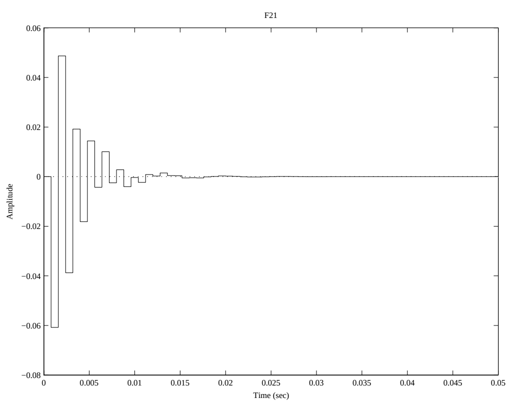

Fig. 16. Impulse response of $F_{21}(z^{-1})$ from L43 to R43.

From Figs. 14 and 16 it can be estimated that the response time from L43 to R43 is within 20 msec, and that the opposite direction from R43 to L43 is about 40 msec. Since these results were obtained from one subject, it is necessary to examine SEF results of more subjects. This will be reported in the near future.

6. CONCLUDION

1) A new way of dynamical understanding of brain function of SEF was proposed by using the decorrelation method of ICA and our blind identification method of transfer functions based on feedback system theory.
2) In SEF stimuli the response time from L43 to R43 was within 20 msec, and the opposite direction from R43 to L43 was about 40 msec. Their directional dependence was found.

7. REFERENCES

[1] K.Kishida: Contraction of Information and Its Inverse Problem in Reactor System Identification, In *Advances in Nuclear Science and Technology*, Lewins and Becker (eds.), vol.**23**, pp. 1-68, Plenum Press, N.Y. (1996).

[2] K.Kishida, H. Fukai, T. Hara and K. Shinosaki, A new approach to blind system identification in MEG data, *IEICE Trans. Fundamentals*, to appear in March 2003.

[3] L. Molgedey and H. G. Schuster, Separation of a mixture of independent signals using time delayed correlations, *Phys. Rev. Lett.*, vol. **72**, pp.3634-3637, 1994.

[4] A. Ziehe, K. R. Müller, G. Nolte, B. M. Mackert and G. Curio, Artifact reduction in Magnetoneurography based on time-delayed second-order correlations, *IEEE Trans. Biomed. Eng.*, vol. **47**, no.1, pp.75-87, 2000.

[5] N. Murata, S. Ikeda and A. Ziehe, An approach to blind source separation based on temporal structure of speech signals, *Neurocomputing*, vol. **41**, pp.1-24, 2001.

[6] T. Allison, G. McCarthy, C.C. Wood, T.M. Darcey, D.D. Spencer and P.D. Williamson, Human cortical potentials evoked by stimulation of the median nerve. I. Cytoarchitectonic areas generating short-latency activity. *J. Neurophysiol.*, vol. **62**, pp. 694-710, 1989.

[7] R. Kakigi, M. Hoshiyama, M. Shimoto, D. Naka, H. Yamasaki, S. Watanabe, J. Xiang, K. Maeda, K. Lam, K. Itomi and A. Nakamura, The somatosensory evoked magnetic fields, *Prog. Neurobiology*, vol. **61**, pp. 495-523, 2000.

[8] J. F. Cardoso and A. Souloumiac, Jacobi angles for simultaneous diagonalization, *SIAM J. Math. Anal. Appl.*, vol. **17**, no. 1, pp.161-164, 1996.

[9] S. Makeig, T. P. Jung, A. J. Bell, D. Ghahremani and T. J. Sejnowski, Blind separation of auditory event-related brain responses into independent components, *Proc. Nat. Acad. Sci. USA*, vol. **94** pp. 10979-10984, 1997.

[10] R. Vigário, J. Särelä, V. Jousmäki, M. Hämäläinen and E. Oja, Independent component approach to the analysis of EEG and MEG recordings, *IEEE Trans. Biomed. Eng.*, vol. **47**, no. 5, pp. 589-593, May 2000.

[11] K. Kishida and N. Suda: A theory of reactor diagnosis in feedback systems, *J. Nucl. Sci. Technol.* vol. **31**, pp. 526-538, 1994.

[12] K. Kishida, Numerical study on identification of transfer functions in a feedback system and model reduction, *J. Nucl. Sci. Technol.* vol.**34**, pp. 1115-1120, 1997.